Radiation Measurements 82 (2015) 14–20

Contents lists available at ScienceDirect

Radiation Measurements

journal homepage: www.elsevier.com/locate/radmeas

Radiation measurements onboard aircraft in the South Atlantic region

C.A. Federico [a,*], O.L. Gonçalez [a], L.V.E. Caldas [b], M.T. Pazianotto [c,a], C. Dyer [d], M. Caresana [e], A. Hands [d]

[a] Institute for Advanced Studies, Applied Physics Department, São José dos Campos, Brazil
[b] Instituto de Pesquisas Energéticas e Nucleares, Comissão Nacional de Energia Nuclear, IPEN/CNEN-SP, São Paulo, SP, Brazil
[c] Aeronautics Technological Institute, Physics Department, São José dos Campos, Brazil
[d] Surrey Space Centre, University of Surrey, Guildford, UK
[e] Politecnico di Milano, Dip. Energia, Milano, Italy

HIGHLIGHTS

- We took measurements of cosmic radiation aboard aircrafts in SAMA region.
- We compared measurements with results from computational codes.
- The flights missions were dedicated for these measurements and very well controlled.

ARTICLE INFO

Article history:
Received 27 March 2015
Received in revised form
22 July 2015
Accepted 24 July 2015
Available online 26 July 2015

Keywords:
Cosmic radiation dose
South Atlantic magnetic anomaly
Flight altitudes
Aircrew

ABSTRACT

There has been considerable research on measurements and simulation of the cosmic radiation doses for aircrew. Most of this was made in the northern hemisphere and on routes between Europe, Asia and North America. The current work shows the results of measurements made onboard a military aircraft specifically in the South Atlantic Anomaly Region, comparing some active and passive instruments and the results from computational dose estimation with special concern about possible effects from the anomaly on the radiation doses.

1. Introduction

Since the discovery of cosmic radiation by Victor Hess, the concerns about their effects on the human lifestyle and equipments have grown continuously. The secondary and tertiary particles, produced by the interaction of the primary cosmic rays in the atmosphere are mainly responsible for the dose deposited in the human body and in electronic equipments. At the altitudes of aircraft flights the main concern is about the dose received by frequent flyers, like the aircrews, and by the probability of malfunction or failure of sensitive equipment as a result of radiation induced faults. At this altitude, the main component of the radiation field, responsible for the most part of the dose and effects on electronics is neutrons.

The ICRP 60 (ICRP, 1991) proposed, in 1990, the inclusion of flight professionals (cabin crew members and pilots) in the group of people to be considered as occupationally exposed to ionizing radiation. The reason for this recommendation is due to the fact that those professionals are usually exposed to radiation levels similarly to the professionals that work with radiation in medicine and technology (Bartlett, 2004). In the usual conditions, the flight professionals can overcome the limit of 1 mSv/year but it is unlikely to overcome the limit of 6 mSv/year.

This recommendation was later described in more detail in subsequent recommendations (ICRP, 1998; ICRP, 2008) that were later adopted by the European Union and Canada. A wider discussion about this subject can be found in the references (Courades, 1999; Federico et al., 2012).

There is special concern relating to some regions of South America due to part of their territory being under the influence of a

* Corresponding author.
E-mail address: claudiofederico@ieav.cta.br (C.A. Federico).

http://dx.doi.org/10.1016/j.radmeas.2015.07.008
1350-4487/

magnetic anomaly called the South Atlantic Anomaly (SAA). In a simplified approximation, one can try to explain this anomaly based on contributions from the displacement and inclination of the dipole, but this is not a true approximation as this hypothesis cannot explain all the behavior of the SAA. A possible contribution for SAA can be related to reversal lava fluxes on the outer Earth core (Hartmann, 2005; Bloxham and Jackson, 1992). The region of SAA can be viewed in Fig. 1, where one can see their region of influence.

Although this anomaly does not necessarily imply a higher dose rate in this region at flight altitudes, its presence changes the way that cosmic radiation interacts with the magnetic field and the atmosphere at higher altitudes, which justifies the need for more studies and more detailed dosimetric assessments.

This work shows the results from flight missions performed on a Brazilian military aircraft with special aim to collect data in the SAA vicinity. It contributes with measurements made exclusively inside this region in very well controlled experimental conditions, which differs from other measurements made in this region, which were made as part of wider flight routes or in less controlled experimental conditions (Vergara and Román, 2009; EURADOS, 2004).

2. Experimental procedure

2.1. Equipment and experimental procedure

The measurements were taken on 7 different flights, performed on LEARJET type aircraft from a Brazilian military flight test group. The flights were fully accompanied with a GPS system, referenced to DATUM WGS84 (Department of Defense, 2000) to ensure the correct altitude and coordinates of each flight.

The measurements were taken by means of two active systems and one passive system, all of them specially calibrated for the atmospheric cosmic-ray radiation field. The calibrations were made in the CERN-EU high energy Reference Field facility (CERF) (Mitaroff and Silari, 2002) at CERN (European Organization for Nuclear Research).

The first active system was a silicon-based dosimeter, developed in the UK and specially designed for measurements on aircraft (RaySure) (Fig. 2). The system is made using PIN type silicon diodes and was previously characterized for this type of field (Dyer et al., 2009; Hands and Dyer, 2009), allowing to obtain the results directly in terms of ambient dose equivalent (H*(10)), which is the recommended quantity for this type of measurement. The solid-state system uses an autonomous power source and the results are obtained in time intervals defined by the user and stored in an internal memory, which can be subsequently read out.

The second system was the THERMO SCIENTIFIC monitor that consists of an acquisition electronics model FH40G-10, with remote acquisition capabilities, programmable by PC, and up to two probes. The system has an internal proportional counter, for measurement of photon radiation, and allows the connection of an external probe with simultaneous acquisition. It was calibrated to present the results directly in the operational quantity H*(10) and stores the values in an internal memory which can be subsequently collected by the user. As external probe, we used one THERMO FHT 762

Fig. 2. The solid-state spectrometer "RaySure" (Dyer et al., 2009; Hands and Dyer, 2009).

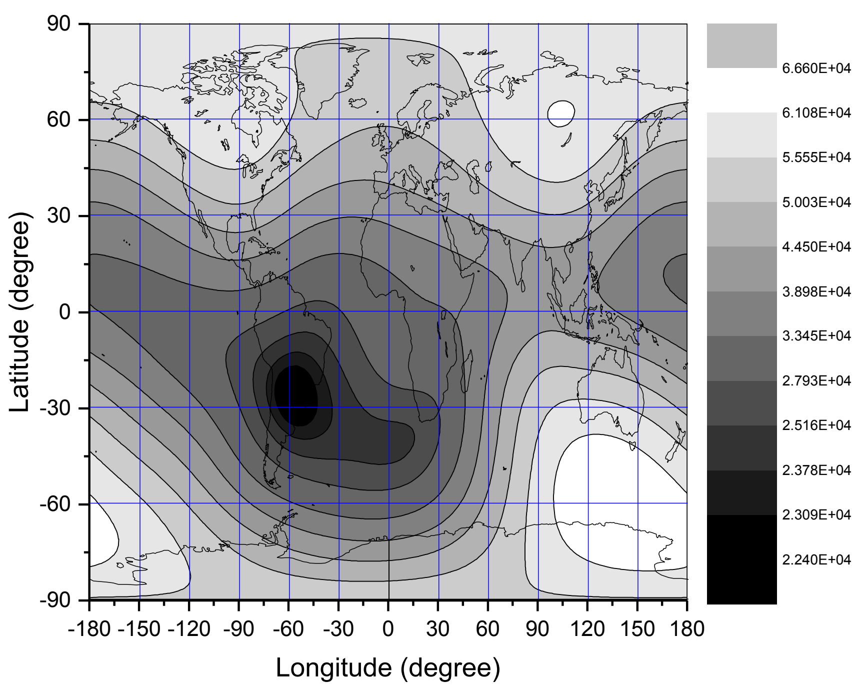

Fig. 1. Map of the geomagnetic field (total intensity, expressed in nT), obtained from IGRF2011 model (IGRF, 2010), for 01 Oct 2010 at 12 km altitude (Federico et al., 2012).

neutron probe, which consists of one ^{3}He proportional counter inside a cylinder made with tungsten and polyethylene layers, projected to obtain the response according to H*(10) for neutrons up to 5 GeV (Thermo-Scientific, 2009). The THERMO FH system can be viewed in Fig. 3 and more details about its calibration can be found in Federico et al. (2013).

The passive dosimetric system, developed at Polytechnic of Milan (Caresana et al., 2007; Agosteo et al., 2010, 2009; Caresana and et al., 2014), consists of one SSNTD (Solid State Nuclear Track Detector) of CR39 PADC (Poly-Allyl-Diglycol-Carbonate), coupled to a ^{10}B enriched converter, positioned inside a sphere made with polyethylene, lead and cadmium, as can be seen in Fig. 4.

This system is based on tracks generated in CR39 PADC by alpha particles from (n,α) reaction on ^{10}B, and its calibration for neutron radiation was previously done in the CERF field, for the operational quantity H*(10).

In all flight measurements these systems were placed every time in the same position on the aircraft, as shown in Fig. 5, to ensure the detection reproducibility.

For all systems, the treatment of uncertainties considered the propagation of calibration uncertainties and also the statistical fluctuation (type A uncertainties) of the measurements, when applicable. Type B uncertainties were not considered because they are difficult to estimate due to lack of knowledge on the influence of several factors on the measurements. Amongst them we can cite the influence of clouds, passengers' motion, fuel distribution between the tanks, short term or regional variations of the cosmic ray field, etc.

2.2. Complete set of missions

The flight measurements were carried out from December 2010 up to June 2011 and were divided between Route Missions (RM), where the aircraft came from one point to another, and Fixed Point missions (FP), where the aircraft performed a circular-type trajectory around specified coordinates, at specified altitudes. Table 1 shows complete information about all the missions.

In Fig. 6 one can see the region covered by these flight missions.

2.3. Computational codes

For comparison purposes, as well as to assess the applicability and reliability in the SAA region, the dose on each mission was also estimated by using free computational codes. The codes used were CARI-6 (EURADOS, 2004), EPCARD (EURADOS, 2004), EXPACS (Sato and Niita, 2006; Sato et al., 2008) for the dose rate estimative in FP missions, the codes AVIDOS (Latocha et al., 2009), CARI-6 and PCAIRE (Lewis et al., 2005) for the route accumulated dose estimation for RM, and the code QARM (Dyer et al., 2007) for the neutron/non-neutron ratio estimative.

Fig. 3. Monitor FH40G-10 with FHT-762 neutron probe.

Fig. 4. Passive dosimetric system, based on CR39 PADC in polyethylene/lead sphere.

3. Results

3.1. Fixed point missions

The results from Fixed Point (FP) missions allow a better control of the measurement uncertainties due to better control of altitude, geographic coordinates and acquisition time. All the FP missions were done with the aircraft stabilized at the designated altitude in a smooth circular orbit around the same coordinate, in order to avoid effects from changes on altitude or geographical coordinates which could interfere with the measurement. Results were fully tracked by an independent GPS system, referred to DATUM WGS84 (Department of Defense (2000)), in order to ensure the real coordinates to be used.

Fig. 7 shows the results obtained on FP missions 1, 2, 3, 4 and 5 (coordinates 22.73 S; 45.46 W, in a flight test area, near São José dos Campos city, SP, Brazil), compared with ones simulated by computational codes EXPACS, EPCARD and CARI-6.

It may be noted that nearly all measurements remain in the ±12.5% interval around the mean of measured and calculated values. This interval corresponds to one relative standard deviation (k = 1), which is the usual variation of any set of good measurements of the H*(10) for atmospheric cosmic radiation as judged by EURADOS's and ICRU's evaluation committees (EURADOS, 2004; ICRU, 2010).

Fig. 8 shows the results from missions 9 and 12 (South of Brazil) where one can see clearly the influence of cut-off rigidity. Special attention shall be paid to mission 9, close to Foz do Iguaçu city, which was chosen due to the proximity to the point of minimum field, in the center of SAA. Here, also, it can be noted that nearly all the values of H*(10) rate lies within the range of ±12%.

The complete set of FP missions, normalized to the mean value of each point is shown in Fig. 9 in order to illustrate the dispersion of the different measurements or calculations. The dashed lines represent the intervals of one standard deviation and two standard deviations. In the same figure one can see an additional point, extracted from a short part of the route mission 7 (Cut-off rigidity 11.2 GV), outside the central region of SAA influence, for comparison purposes, due to its higher cut-off rigidity.

Similarly to Fig. 7, this figure shows that most of the normalized values for H*(10) rate remain within the range of one relative standard deviation, and almost of all remain within two standard deviations (95% probability). This shows that, according to what has been established by ICRU and EURADOS, both set of measured

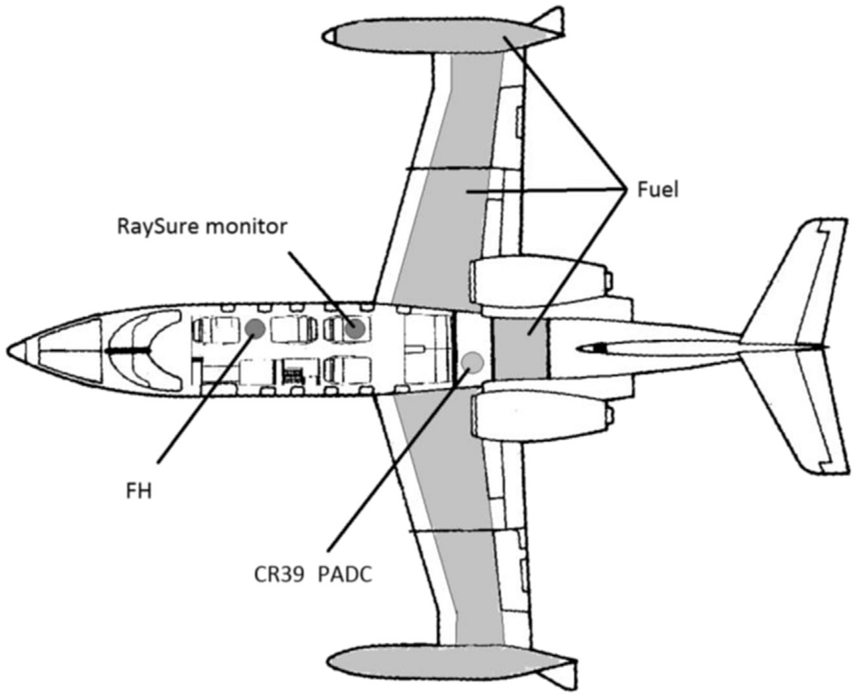

Fig. 5. Active and passive instruments positions, inside aircraft.

Table 1
Resume of flight missions.

No.	Type	Geographic coordinates	Date	Hour (UT)	Altitude (m) and [flight level]
1	FP	22.73 S; 45.46 W	08 Dec 2010	17:00 18:00	4876 [FL 160]
2	FP	22.73 S; 45.46 W	11 Mar 2011	11:00 12:00	7010 [FL 230]
3	FP	22.73 S; 45.46 W	30 Dec 2010	14:00 15:00	9448 [FL 310]
4	FP	22.73 S; 45.46 W	30 Dec 2010	15:00 16:00	10,668 [FL 350]
5	FP	22.73 S; 45.46 W	11 Mar 2011	12:00 13:00	13,106 [FL 430]
6	RM	23.13 S; 45.51 W to 08.07 S; 34.55 W	23 Mar 2011	08:30 12:16	10,058 (mean)
7	RM	08.07 S; 34.55 W to 23.13 S; 45.51 W	24 Mar 2011	20:34 23:36	10,180 (mean)
8	RM	23.13 S; 45.51 W to 26.00 S; 53.30 W	29 Jun 2011	11:46 13:33	13,157 (mean)
9	FP	26.00 S; 53.30 W	29 Jun 2011	13:33 14:33	12,496 [FL 410]
10	RM	23.00 S; 53.30 W to 29.95 S; 51.15 W	29 Jun 2011	14:33 15:13	11,887 (mean)
11	RM	29.94 S; 51.15 W to 31.33 S; 50.79 W	29 Jun 2011	17:38 18:17	up to 12,497
12	FP	31.25 S; 50.75 W	29 Jun 2011	18:17 19:36	12,192 [FL 400]
13	RM	31.25 S; 50.75 W to 23.13 S; 45.51 W	29 Jun 2011	19:36 21:01	12,496 [FL 410]

values and the calculated ones by computer codes are consistent one with the other.

In order to see any possible behavior on the radiation dose rates inside the SAA region, Fig. 10 compares the measured H*(10) rates and the mean values of computational estimative of H*(10) rates, as a function of distance from SAA center, for high altitude missions (>10,800 m). The SAA center was estimated for 2010, using the criteria of the minimum field strength, from data obtained from Hartmann (Hartmann, 2005) and the coordinates obtained were 27.0 S, 56.5 W.

In Fig. 11 one can see the ratio between non-neutronic and neutronic components of the field. In the same figure one can see, for comparison purposes, two points taken from Romero et al. (2004), for similar altitudes and cut-off rigidities and for similar measurement equipments (Romero et al., 2004). The equipment used by Romero et al. was composed by a SWENDI2 neutron probe, very similar to the THERMO FH 762 used in this work, and the non-neutron probe used by Romero et al. was an ionization chamber

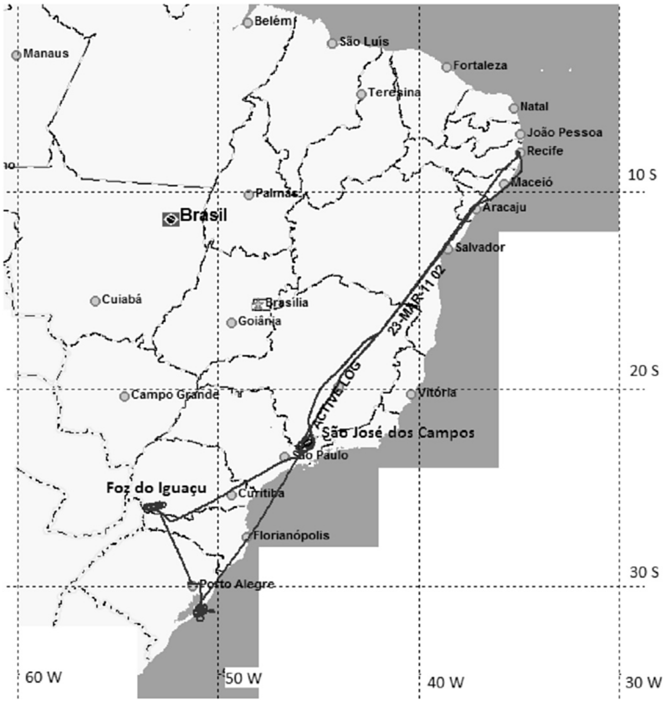

Fig. 6. Visualization on the region covered by the flight missions.

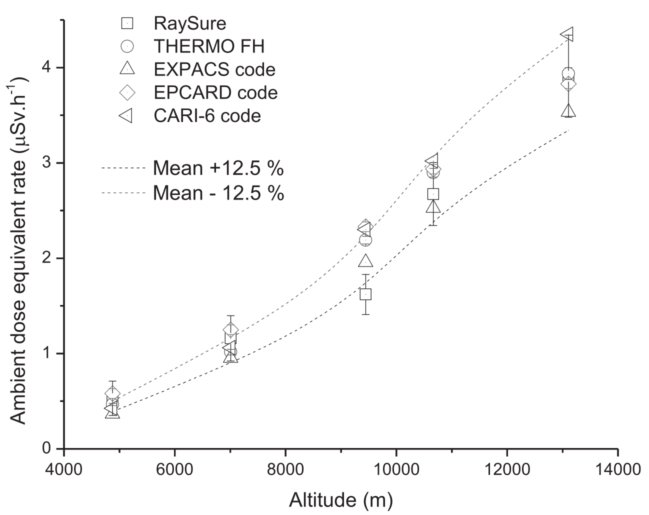

Fig. 7. Results for missions 1, 2, 3, 4 and 5, performed near São José dos Campos city, Brazil (9.6 GV cut-off rigidity). The dashed curves correspond to a fitting of the mean of values (measurements plus computational calculation) on each altitude ± 12.5%, only to allow visual guidance.

RSS131 and a proportional counter was used in this work.

The difference between the measurement and simulation values appears to be related with the equipment used, which are similar. As a first order analysis, this divergence could be explained due to the response function of the neutron probe of the equipment, which presents a slightly underestimation for neutron energies between 7 and 80 MeV. Romero et al. (2004) observed the same behavior and suggested some overestimation on non-neutron probe measurements, over the neutron measurements. This behavior needs to be more investigated.

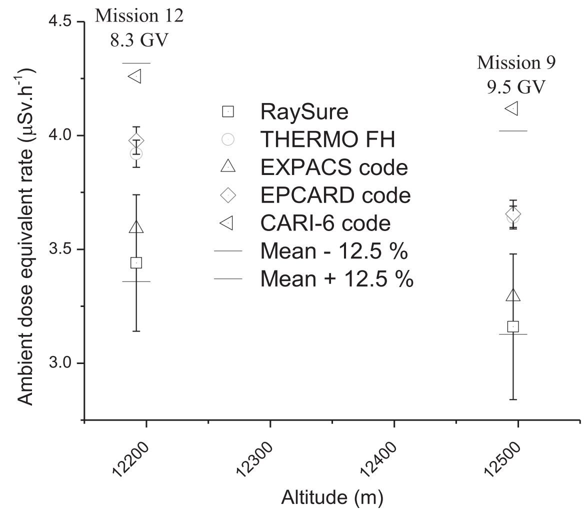

Fig. 8. Measurements from missions 9 and 12.

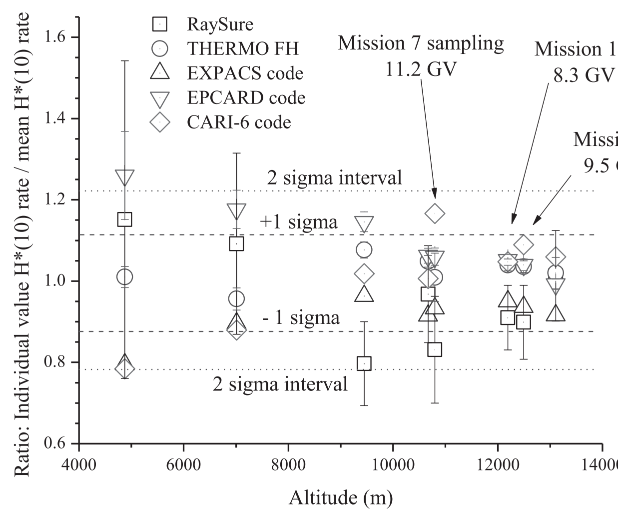

Fig. 9. Measured/mean H*(10) ratio, for the complete set of fixed–point missions, with inclusion of one sampling extracted from mission 7. The points without information were made at 9.6 GV cut-off rigidity.

3.2. Route missions

The whole set of route missions are summarized in Fig. 12 in terms of effective dose for the measurements taken by the active instruments. The mean deviation interval for the whole set of values (measured plus computationally estimated) were within 22%, if we do not consider AVIDOS estimates, which are clearly out of data set, the mean deviation interval falls between 13%. The uncertainties related on AVIDOS estimates are related to the fact that the most part of missions have short pathways (hundreds of km) and the graphical interface of AVIDOS code did not allow good precision in this situation.

For the route missions, most part of the codes gives the results in terms of Effective dose (E), in order to be easily compared with the dose limits. In this case, the experimental results obtained in terms of H*(10) were converted to E according the conversion factors suggested by ICRU 84 (2010) (ICRU, 2010).

The passive measurements were taken cumulatively by PADC dosimeter during the missions 6 and 7 and during the missions 8 to 13. The results are shown in Fig. 13, compared with cumulative

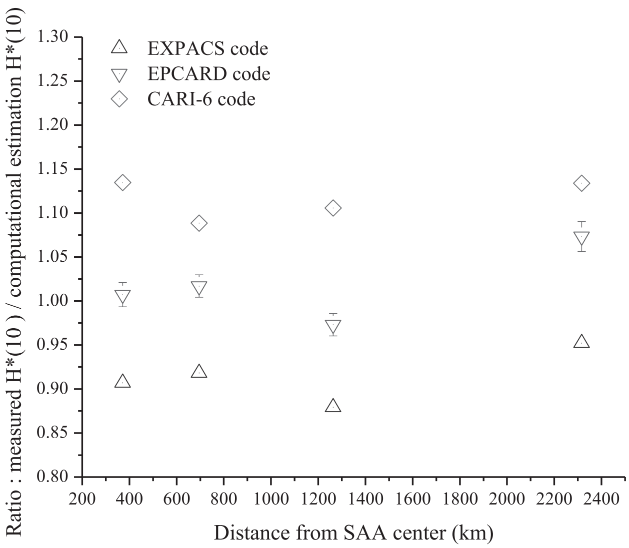

Fig. 10. Comparison of the mean of the measured H*(10) rates and the computational estimative of H*(10) rates in function of the distance from SAA.

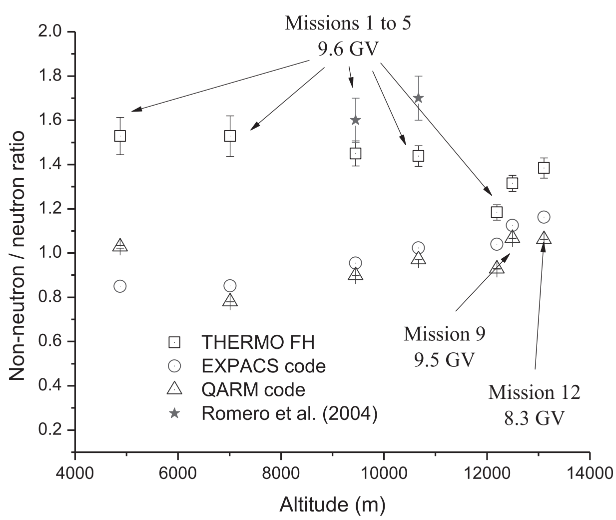

Fig. 11. Non-neutron/neutron ratio, for different FP missions, in comparison with Romero et al. (Romero et al., 2004).

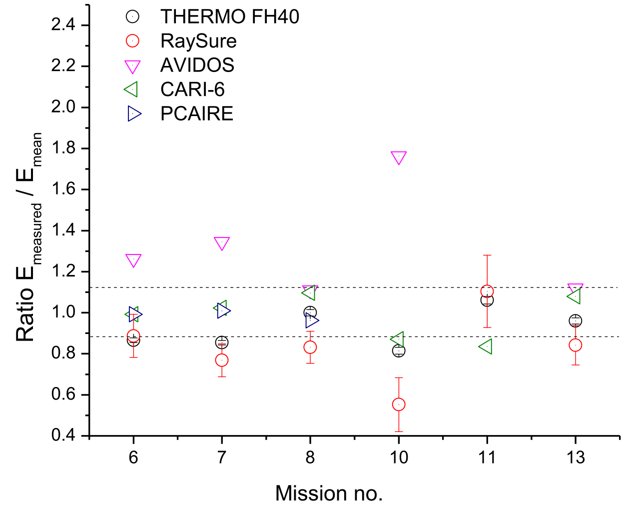

Fig. 12. Measured/mean E ratio, for the complete set of route missions. The dashed lines corresponds to the typical interval of ±12.5%, only for visual guidance.

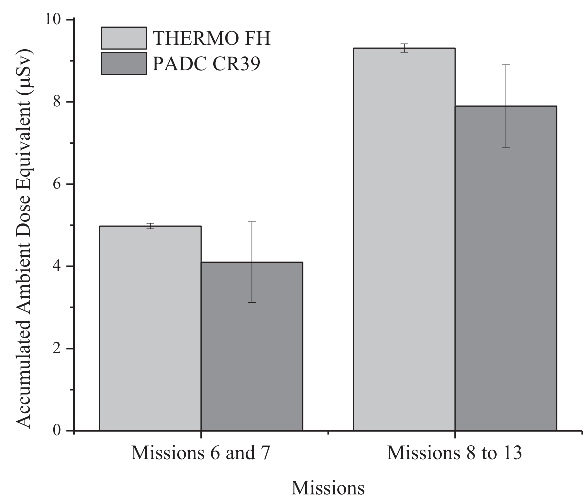

Fig. 13. Cumulative measurements of the neutron component taken from PADC CR-39 dosimeter and from the FHT-762 neutron probe.

measurements from the FH neutron probe. The large differences between the integrated dose from missions 6 and 7 (around 4–5 μSv) and missions 8 to 13 (around 8–9 μSv), could be explained by the low altitudes and equatorial latitudes of missions 6 and 7 (around 10 km altitude and 23° S to 8° S latitudes), compared with missions 8 to 13 (between 11 km and 13 km altitudes and 23° S to 31° S latitudes).

3.3. Geomagnetic and solar conditions

The solar and geomagnetic conditions can affect the cosmic radiation. These effects need to be considered to allow the comparison between experimental and computational results. The most important factors to evaluate the solar and geomagnetic conditions are the Heliocentric potential, which represents the result of a steady-state solution to the diffusion equation of cosmic rays through the solar wind and is deduced from neutron monitors output (O'Brien et al., 2005) and the Kp index, which quantifies disturbances in the horizontal component of earth's magnetic field with an integer in the range 0–9 with 1 being calm and 5 or more indicating a geomagnetic storm.

The solar and geomagnetic parameters considered during these missions are shown in Table 2, where the Cut-off rigidity was computed by using the QARM code, the geomagnetic perturbation index Kp was obtained from GFZ (Adolf-Schmidt-Observatory Niemegk) (GFZ, 2011) and the heliocentric potential, for each specific date and time, was obtained from direct consultation of FAA (US Federal Aviation Administration). One can see that the Kp index was always ≤3. The proton flux was also verified by means of the data obtained from GOES satellites (SWPC, 2011) and shows no sensitive variations during the missions (i.e. no Solar Particle Events (SPE) or ground level radiation effect of SPE).

4. Conclusions

Radiation measurements aboard aircraft during flight routes between airports were performed, as well as flight around the same geographical coordinate (Fixed Point) and the same altitude. It is should be emphasized that the missions were dedicated to this

Table 2
Solar and geomagnetic parameters of flight missions.

Mission	Cut-off rigidity (GV)	Heliocentric potential (MV)	Kp index
1	9.6	382	3
2	9.6	411	2
3	9.6	374	1
4	9.6	397	2
5	9.6	411	2
6	from 9.6 to 11.7	384	3
7	from 11.7 to 9.6	364	1
8	From 9.6 to 9.5	502	0
9	9.5	502	0
10	from 9.5 to 8.6	502	1
11	from 8.6 to 8.3	502	1
12	8.3	502	1
13	from 8.3 to 9.6	502	1

study with rigorous monitoring, which allowed a rigorous evaluation in this geographic region that is subject to the possible effects of the SAA.

The experimental results, when compared to the estimates obtained using the computer code CARI-6 (EURADOS, 2004), EPCARD (EURADOS, 2004), EXPACS (Sato and Niita, 2006; Sato et al., 2008) for the dose rate in estimative FP missions and the codes AVIDOS (Latocha et al., 2009), CARI6 and PCAIRE (Lewis et al., 2005) for accumulated dose estimation in the route for RM, show that the computational estimates present a good agreement with the measurements considering the typical and acceptable uncertainties.

In measurements at a fixed point at different distances from the SAA center (Fig. 10), it was observed that there was no observable systematic effect, confirming that there is not influence of the SAA on the radiation dose at flight altitude, at least in calm solar and magnetospheric conditions. The results do not allow concluding if there are any types of influence of the SAA in extreme disturbed solar and magnetospheric conditions which could be the subject for future investigation.

The comparison of the measurements between the THERMO-FH system and dosimeter based on CR-39 shows a reasonable agreement with a slight underestimation of the latter, demonstrating its viability for evaluation of H*(10) in routes.

Finally, it should be emphasized that it is the first comprehensive work made with this kind of approach with the participation of a group of South American researchers and it is also one of the few that made it using a small and dedicated aircraft to this kind of study.

For future work, we intend to increase the number and diversity of measurements as well as covering situations of solar and magnetospheric disturbance in this region.

Acknowledgment

The authors thanks to CERN and to Dr. Marco Silari and Dr. Markus Brugger for the support on calibration of part of equipment on CERF field. The authors thank also the aircrew and staff from Institute for Research and Flight Tests (IPEV), from Brazilian Air Force, due to support on the measurements inside aircraft. The author's thanks to Dr. Kyle Copeland (FAA), for the information about the heliocentric potential on specific dates and times. The author's thanks also to CNPQ (process 402209/2013-3 and 481432/2013-2) and FINEP (CITAR project, covenant 01.12.0224.00), for the partial financial support.

References

Agosteo, S., Caresana, M., Ferrarini, M., Silari, M., 2009. A passive rem counter based on CR39 SSNTD coupled with a boron converter. Radiat. Meas. 44, 985–987.

Agosteo, S., Caresana, M., Ferrarini, M., Silari, M., 2010. A dual-detector extended range rem-counter. Radiat. Meas. 45, 1217–1219.

Bartlett, D.T., 2004. Radiation protection aspects of the cosmic radiation exposure of aircraft crew. Radiat. Prot. Dosim. 109 (4), 349–355.

Bloxham, J., Jackson, A., 1992. Time-dependent mapping of the magnetic field at the core-mantle boundary. J. Geophys. Res. Solid Earth 97, 19537–19563.

O'Brien, K., Felsberger, E., Kindl, P., 2005. Application of the heliocentric potential to aircraft dosimetry. Radiat. Prot. Dosim. 116 (1–4), 336–342.

Caresana, M., et al., 2014. Calibration of a Passive Rem Counter with Monoenergetic Neutrons, Radiation Measurements. http://dx.doi.org/10.1016/j.radmeas.2014.07.019.

Caresana, M., Agosteo, S., Campi, F., Ferrarini, M., Porta, A., Silari, M., 2007. Sensitivity study of CR39 track detector in an extended range Bonner sphere spectrometer. Radiat. Prot. Dosim. 126 (1–4), 310–313.

Courades, J.M., 1999. European legislation on protection against cosmic radiation. Radiat. Prot. Dosim. 86 (4), 343–346.

Department of Defense, 2000. World Geodetic System 1984, its Definition and Relationships with Local Geodetic Systems. NIMA Technical Report 8350.2. Third Edition, amendment 1.

Dyer, C., Lei, F., Hands, A., Truscott, P., August 2007. Solar particle events in the QinetiQ atmospheric radiation model. IEEE Trans. Nuc. Sci. 54 (4).

Dyer, C., Hands, A., Lei, F., Truscott, P., Ryden, K., Morris, P., Getley, I., Bennett, L., Bennett, B., Lewis, B., 2009. Advances in measuring & modelling the atmospheric radiation environment. IEEE Trans. Nucl. Sc. 56 (6).

EURADOS, 2004. Cosmic Radiation Exposure of Aircraft Crew. European Radiation Dosimetry Group (Radiation Protection 140, Final Report of EURADOS Work Group 5).

Federico, C.A., Gonçalez, O.L., Sordi, G.M.A.A., Caldas, L.V.E., Apr.-Jun., 2012. Effects of cosmic radiation in aircrafts: a discussion about aircrew over south america. J. Aerosp. Technol. Manag. São José Dos. Campos 4 (2), 219–225.

Federico, C.A., Gonçalez, O.L., da Fonseca, E.S., Patrão, K.C.S., Pereira, M.A., Caldas, L.V.E., 2013. Verification of response of neutron monitor for in-flight neutron dosimetry. J. Aerosp. Technol. Manag. (Online) 5, 315–322.

GFZ. Deutsches GeoForschungsZentrum. Historical tables. Available at: <ftp://ftp.gfz-potsdam.de/pub/home/obs/kp-ap/tab/>. access on 12.03.11.

Hands, A., Dyer, C., 2009. Technique for measuring dose equivalent and neutron fluxes in radiation environments using silicon diodes. IEEE Transac. Nuc. Sci. 56 (6).

Hartmann, G.A., 2005. A Anomalia Magnética do Atlântico Sul: Causas e Efeitos. Instituto de Astronomia, Geofísica e Ciências Atmosféricas da Universidade de São Paulo, São Paulo, Brazil. Master Thesis (in Portuguese).

ICRP. International Commission on Radiological Protection, 1991. Recommendations of the international commission on radiological protection. Ann. ICRP 21, 1–3. Publication 60.

ICRP. International Commission on Radiological Protection, 1998. General principles for the radiation protection of workers. Ann. ICRP 27 (1). Publication 75.

ICRP. International Commission on Radiological Protection, 2008. The 2007 recommendations of the international commission on radiological protection. Ann. ICRP 37, 2–4. Publication 103.

ICRU. International Commission on Radiation Units and Measurements, 2010. Reference data for the validation of doses from cosmic-radiation exposure of aircraft crew. J. ICRU 10 (2). ICRU Report 84.

IGRF. International Association of Geomagnetism and Aeronomy, December 2010. International geomagnetic reference field: the eleventh generation. WORKING GROUP V-MOD Geophys. J. Int. 183 (Issue 3), 1216–1230. http://dx.doi.org/10.1111/j.1365-246X.2010.04804.x, 2010.

Latocha, M., Beck, P., Rollet, S., 2009. AVIDOS - a software package for european accredited aviation dosimetry. Radiat. Prot. Dosim. 136 (1–4), 286–290.

Lewis, B.J., Bennett, L.G.I., Green, A.R., Butler, A., Desormeaux, M., Kitching, F., Maccall, M.J., Ellaschuk, B., Pierre, M., 2005. Aircrew dosimetry using predictive code for aircrew radiation exposure (PCAIRE). Radiat. Prot. Dosim. 116 (1–4), 320–326.

Mitaroff, A., Silari, M., 2002. The CERN-EU high-energy reference field (CERF) facility for dosimetry at commercial flight altitudes and in space. Radiat. Prot. Dosim. 102 (1), 7–22.

Romero, A.M., Saez-Vergara, J.C., Rodriguez, R., Domínguez-Mompell, R., 2004. Study of the ratio of non-neutron to neutron dose components of cosmic radiation at typical commercial flight altitudes. Radiat. Prot. Dosim. 110 (1–4), 357–362.

Sato, T., Niita, K., 2006. Analytical functions to predict cosmic-ray neutron spectra in the atmosphere. Radiat. Res. 166, 544–555.

Sato, T., Yasuda, H., Niita, K., Endo, A., Sihver, L., 2008. Development of PARMA: PHITS-based analytical radiation model in the atmosphere. Radiat. Res. 170, 244–259.

SWPC. Space Weather Prediction Center. National Weather Service. Historical plots. Available at: <http://www.swpc.noaa.gov/ftpmenu/plots.html>. accessed 08.05.11.

Thermo-Scientific, 2009. FHT 762- WENDI-2 Datasheet, n.42540/85 TD-e.

Vergara, J.C.S., Román, R.D., 2009. The implementation of cosmic radiation monitoring in routine flight operation of Iberia Airline of Spain: 1 Y of experience of in-flight permanent monitoring. Radiat. Prot. Dosim. 136 (4), 291–296.